Supporting Information for

Bioinspired MXene-Based User-Interactive Electronic Skin for Digital and Visual Dual-Channel Sensing

Wentao Cao[1, 2], Zheng Wang[1], Xiaohao Liu[1], Zhi Zhou[1], Yue Zhang[1],Shisheng He[1, *], Daxiang Cui[1, 2, 3, *], Feng Chen[1, *]

[1]Department of Orthopedic, Spinal Pain Research Institute, Shanghai Tenth People's Hospital, School of Medicine, Tongji University, Shanghai 200072, P. R. China

[2]National Engineering Research Center for Nanotechnology, Shanghai 200241, P. R. China

[3]Institute of Micro-Nano Science and Technology, School of Electronic Information and Electrical Engineering, Shanghai Jiao Tong University, Shanghai 200240, P. R. China

*Corresponding authors. E-mail: fchen@tongji.edu.cn (Feng Chen); tjhss7418@tongji.edu.cn (Shisheng He); dxcui@sjtu.edu.cn (Daxiang Cui)
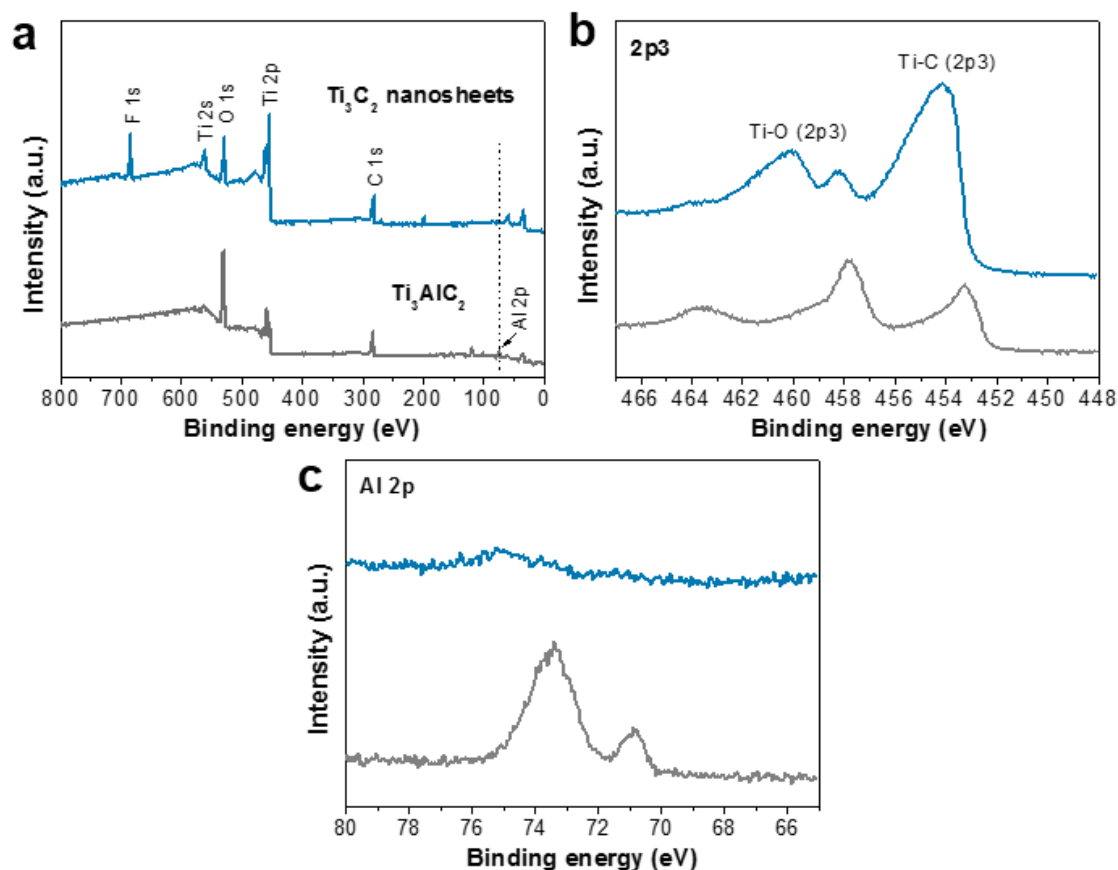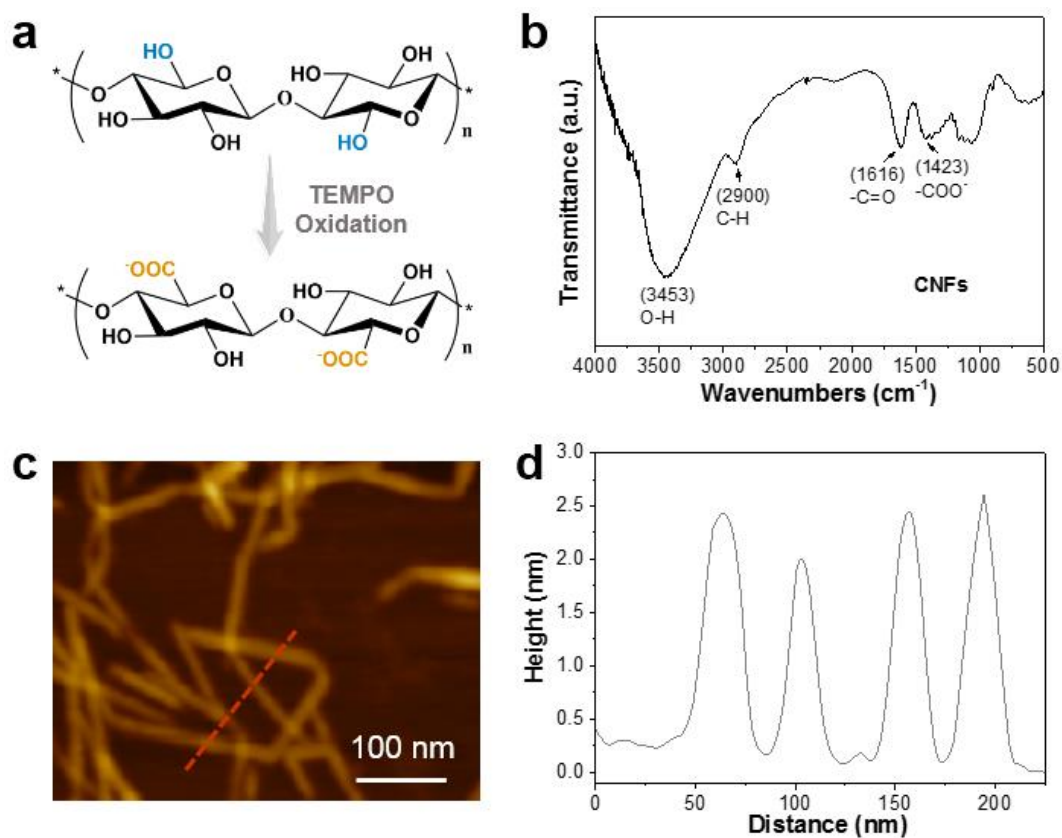
Supplementary Figures
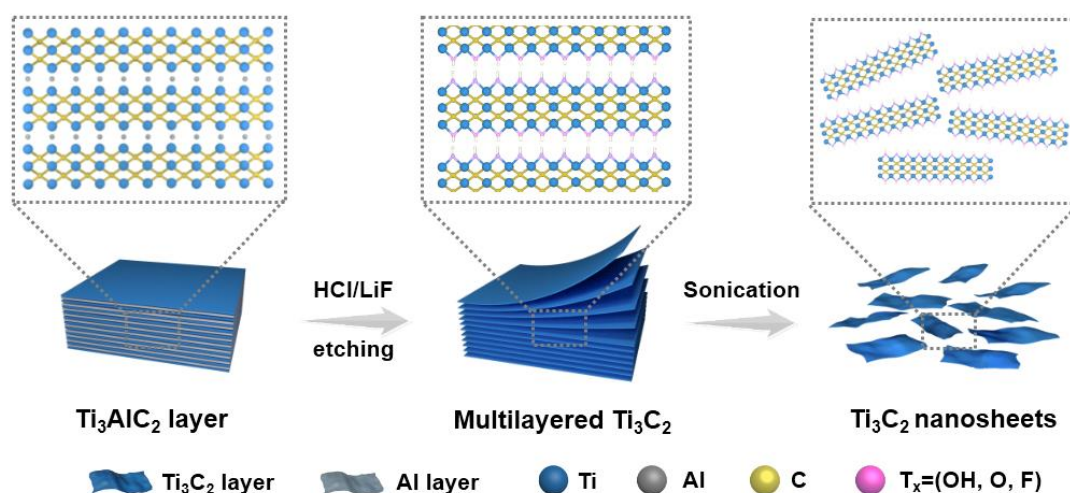
Fig. S1 Schematic for the synthesis of Ti_3C_2 MXene
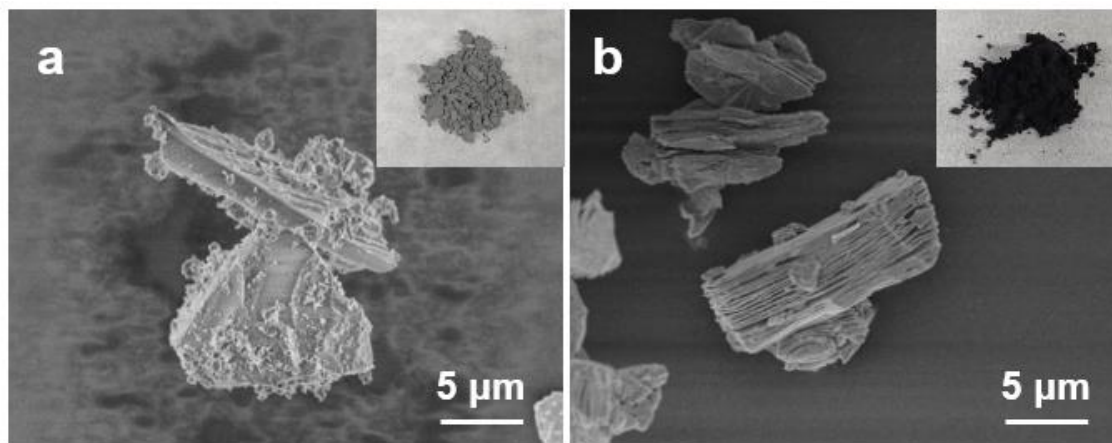
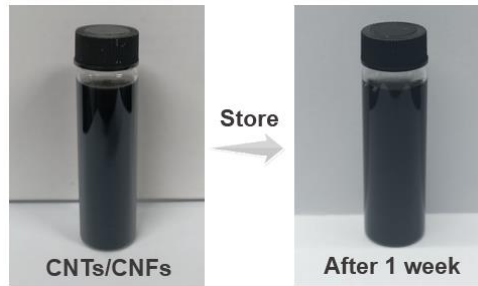**Fig. S2** SEM images of (**a**) Ti_3AlC_2 and (**b**) accordion-like multilayered MXene

Fig. S3 (**a**) XPS survey, (**b**) Ti 2p, and (**c**) Al 2p spectra of Ti_3AlC_2 precursor and Ti_3C_2 MXene nanosheets
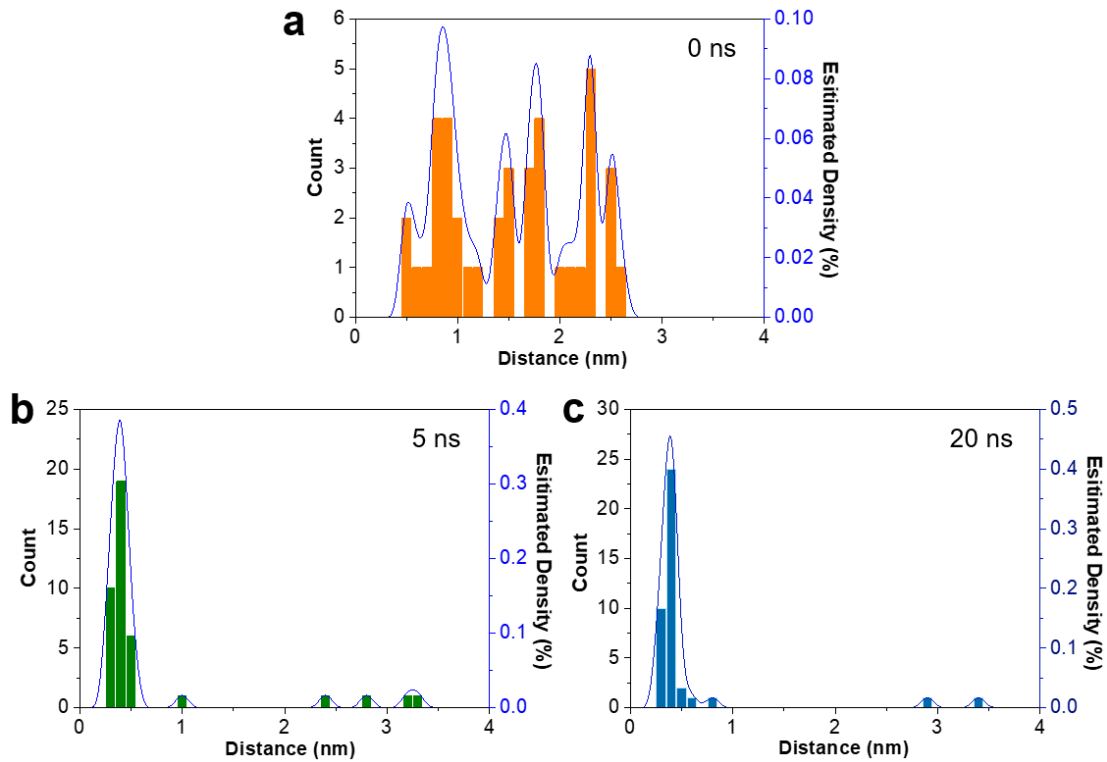

Fig. S4 (**a**) Schematic of the TEMPO oxidation process to prepare CNFs. (**b**) FTIR spectra, (**c**) AFM image, and (**d**) height profiles of CNFs
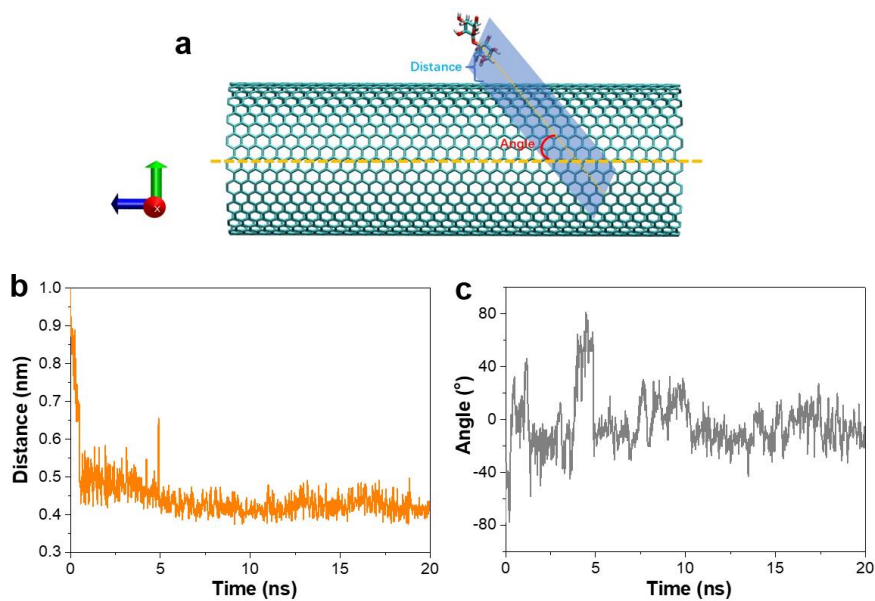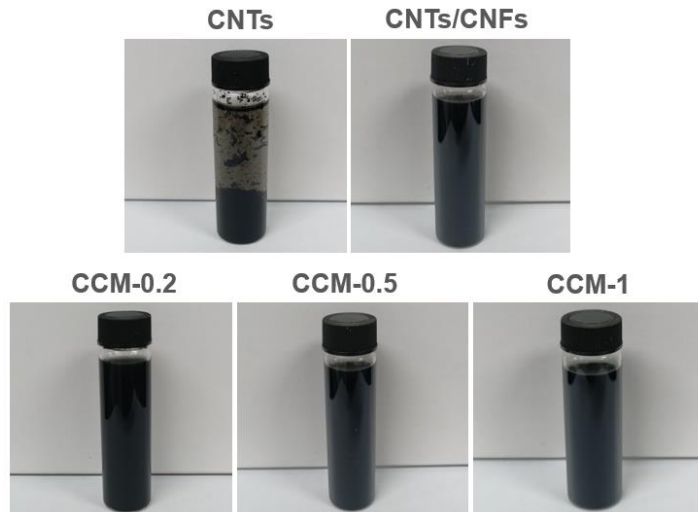
Fig. S5 CNTs/CNFs solution stability test over a week

Fig. S6 Histograms and estimated densities of the distance between the atoms of glucose and the surface of CNT at (**a**) 0, (**b**) 5, and (**c**) 20 ns
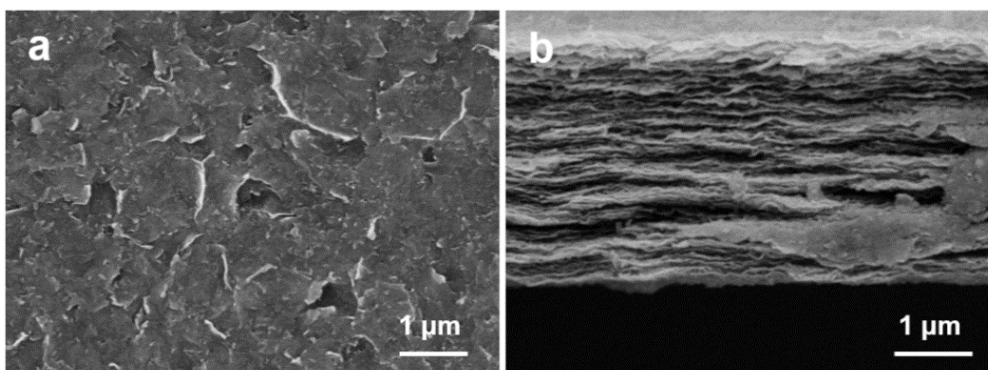

Fig. S7 (**a**) Definition of the parameters between glucose and CNT. Evolution of (**b**) the distance and (**c**) the angle between glucose and CNT
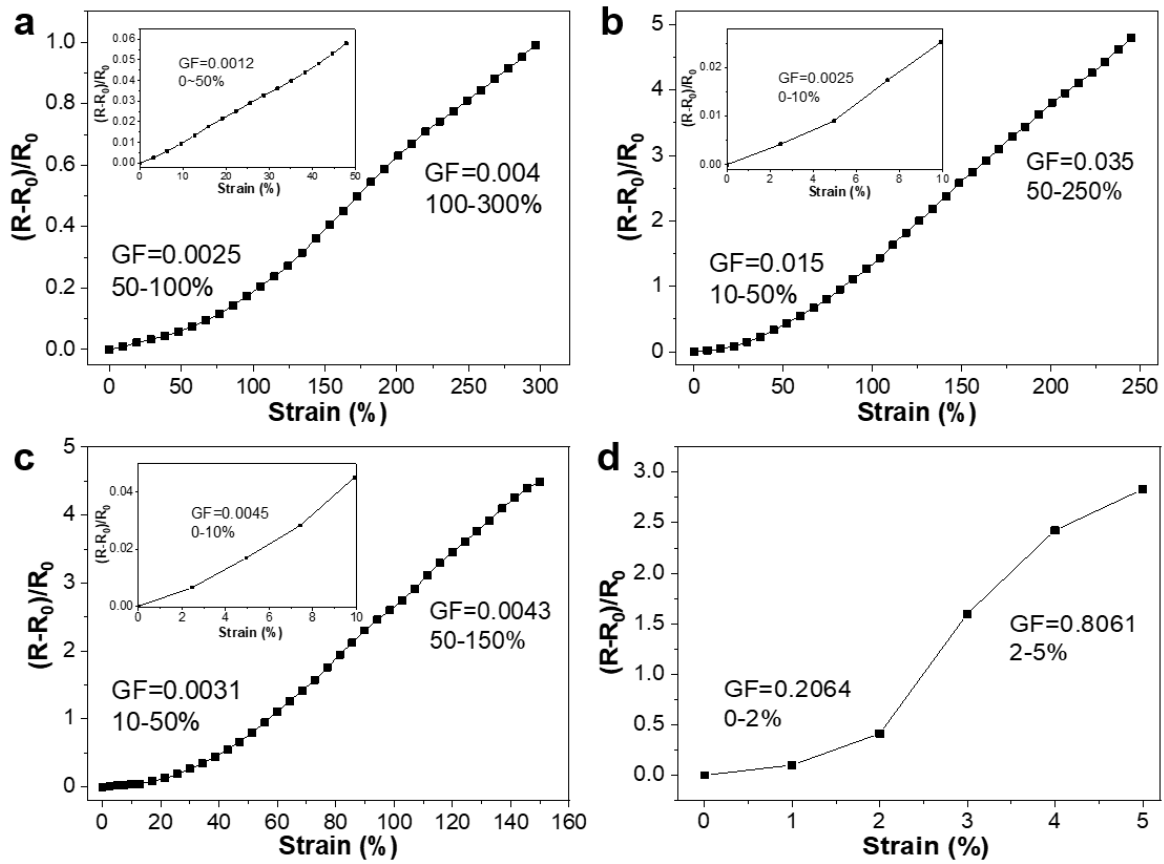
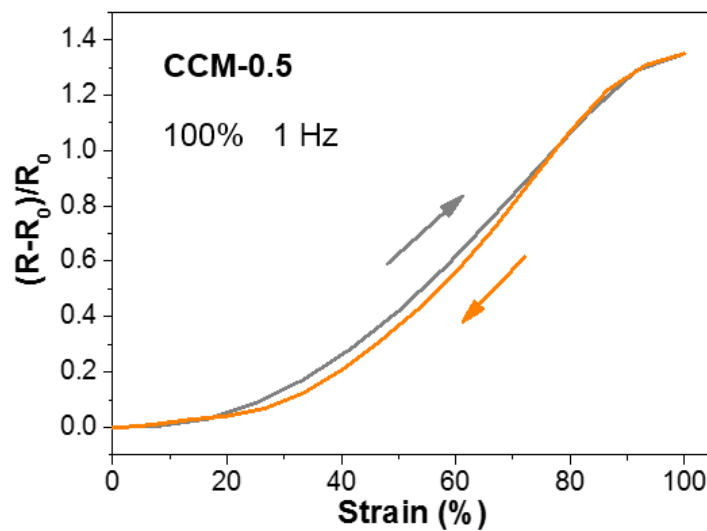**Fig. S8** Digital photographs of CNTs, CNTs/CNFs, and CCM dispersion
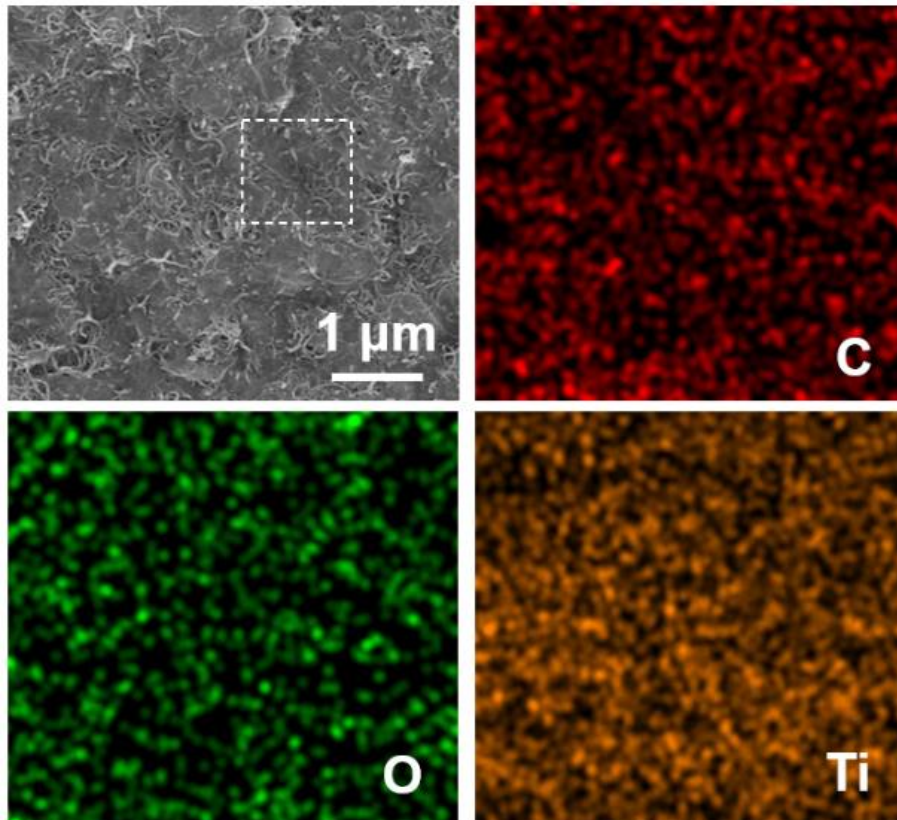
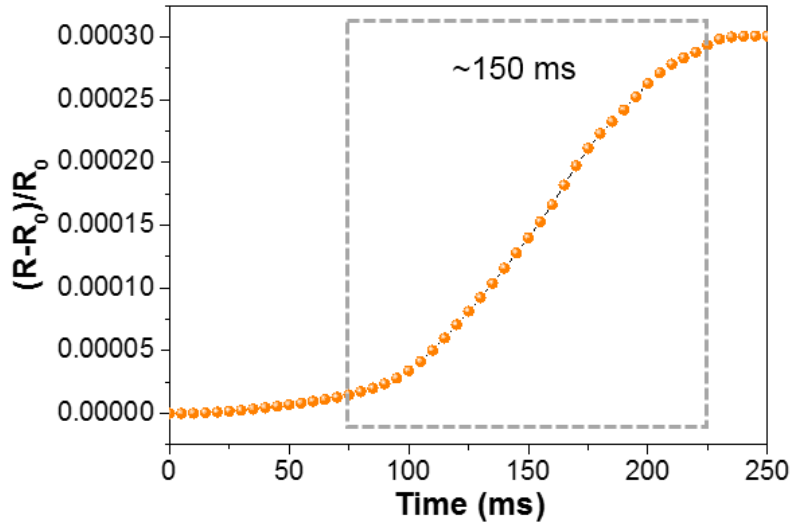**Fig. S9** EDS elemental mapping image of the CCM film


Fig. S10 (**a**) Top-view and (**b**) cross-sectional c

Fig. S11 The GF and linear behavior of (**a**) CNFs/CNTs, (**b**) CCM-0.5, (**c**) CCM-1, and (**d**) pristine MXene e-skin
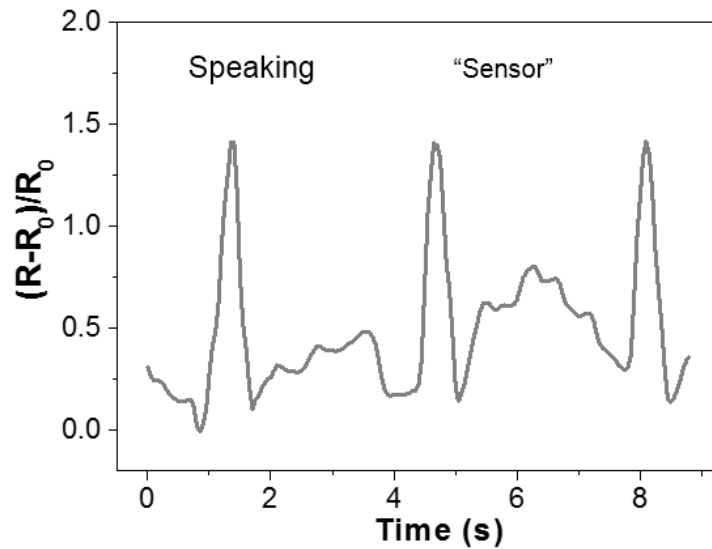

Fig. S12 Typical relative resistance changes versus applied strain curves under one stretch and release cycle for the CCM-0.5 e-skin at a frequency of 1 Hz under 100% strain
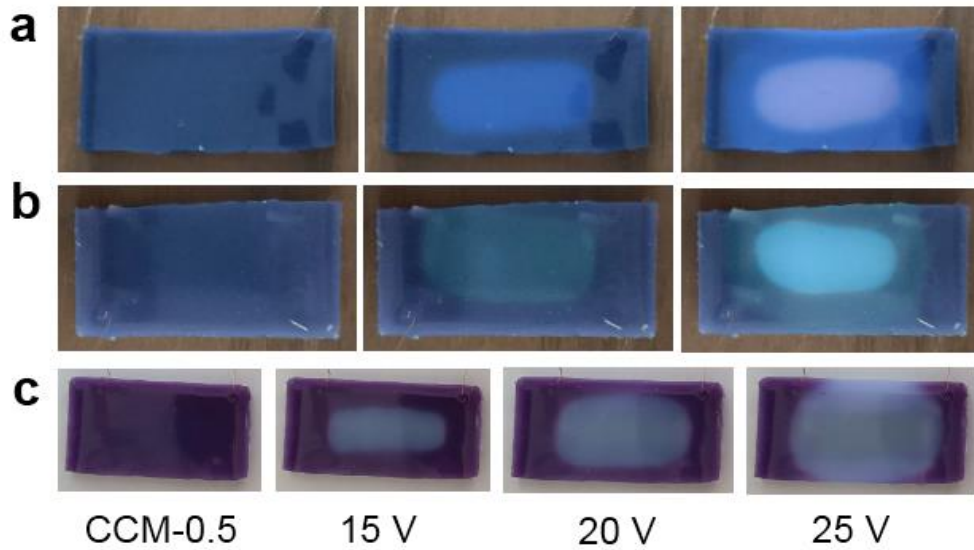
**Fig. S13** Relative resistance changes of the CCM-0.5 e-skin under a quasi-transient step strain of 0.5%
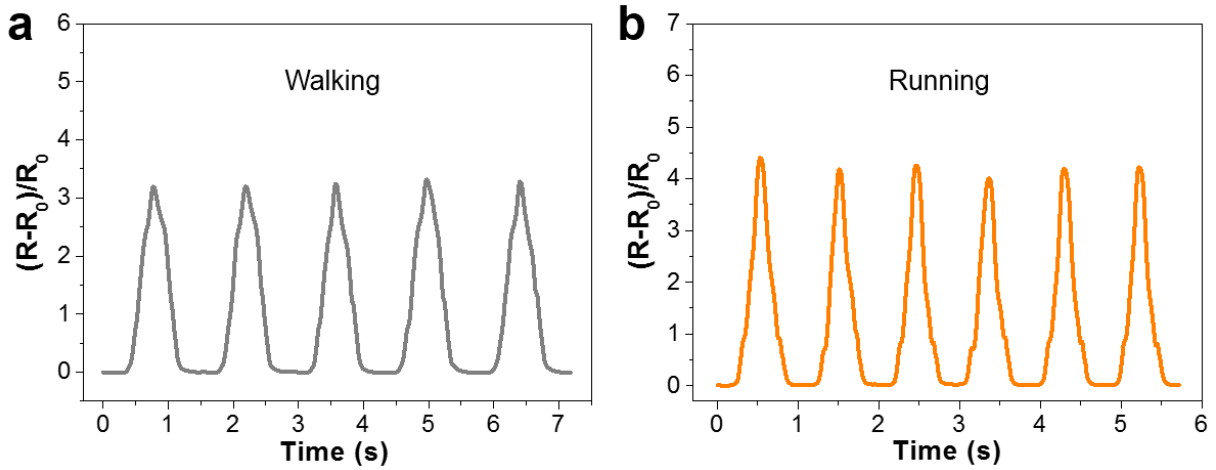
Fig. S14 Responsive curves of the CCM-0.5 e-skin on the knee under motions of (**a**) walking and (**b**) running

Fig. S15 Responsive curve recorded during speaking "sensor"

Fig. S16 (**a**) Photographs of a sample with black and blue pigments that change color in response to an applied voltage of 20 V. (**b**) Photographs of a sample with black and purple pigments that change color in response to an applied voltage of 20 V. (**c**) Photographs of a sample with purple pigments that change color in response to various applied voltage
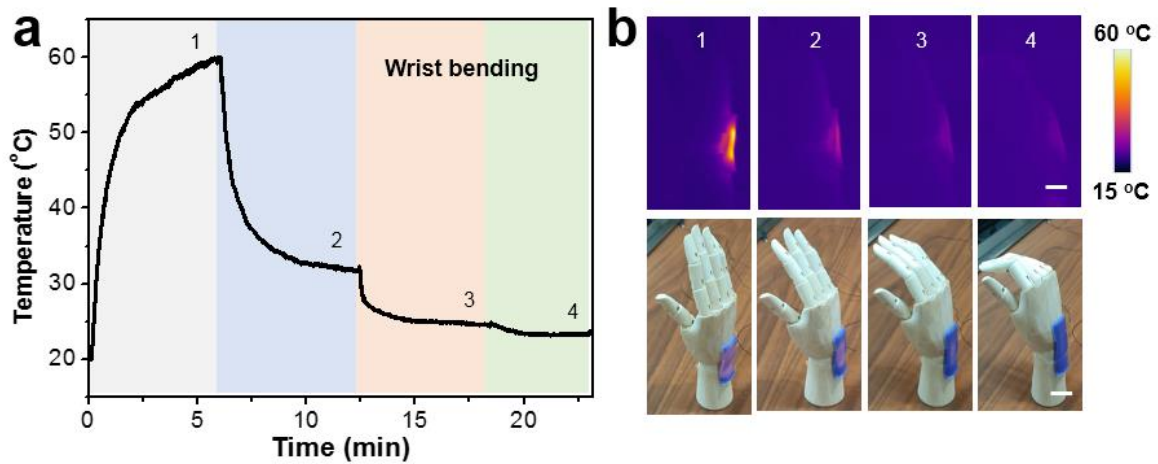
Fig. S17 (**a**) Temperature variations of the CCM e-skin with gradually bending of wrist. (**b**) Photographs and corresponding temperature mapping of wrist under different states of motion in a) (scale bar: 2 cm)